9-2004

Dissolution, Reactor, and Environmental Behavior of ZrO2-MgO Inert Fuel Matrix: Neutronic Evaluation of ZrO2-MgO Inert Fuels

E. Fridman
Ben-Gurion University of the Negev

A. Galperin
Ben-Gurion University of the Negev

E. Shwageraus
Ben-Gurion University of the Negev

Dissolution, Reactor, and Environmental Behavior of ZrO_2-MgO Inert Fuel Matrix

Neutronic Evaluation of MgO-ZrO2 Inert Fuels

Progress Report

Prepared by Reactor Analysis Group
Department of Nuclear Engineering
Ben-Gurion University of the Negev
Beer-Sheva, Israel

July-September 2004

E. Fridman, A. Galperin, E. Shwageraus,

Contents:

List of Figures:

List of Tables:

Task 1: Benchmark of computational tools

I. Introduction

This progress report presents results of analysis performed within the framework of "Dissolution, Reactor, and Environmental Behavior of ZrO_2-MgO Inert Fuel Matrix" project managed by University of Nevada at Las Vegas, Harry Reid Center for Environmental Studies.

The BGU working program includes the following four tasks:

1. Benchmark of computational tools
2. Determination of fissile Pu loading
3. Evaluation of burnable poison designs
4. Evaluation of reactivity feedback coefficients

This progress report presents the results of Task 1. The main objective of this task is to confirm the validity of the ELCOS [1] code system for inert matrix fuel analysis applied to a standard PWR fuel design. Computer codes used are described briefly in the subsequent section. We performed a series of benchmark calculations, which were designed to include the possible range of fuel compositions.

We considered a unit fuel cell and 2-D fuel assembly geometries. The main computer code of the ELCOS system for assembly calculations – BOXER [2], was tested against MCNP code with two different cross-section libraries.

II. Description of Computer Codes

This section presents a brief description of the codes used in this benchmark. The main part of the BGU working program is planned to be performed with ELCOS system.

BOXER is a modular code for two-dimensional neutron transport calculation of LWR fuel lattices. The main modules of the code are:

Cell calculation module

In every configuration to be treated, the most important cell from the point of view of the neutron spectrum is chosen as the "principal cell type". It is calculated with white boundary conditions. Its outgoing partial currents can be used as boundary conditions for other cell types and for the homogeneous materials. The cell calculation begins with the resonance calculation in two material zones and about 8000 lethargy points depending on the composition of the material, employing collision probability method. The resulting ultra fine spectrum is used as weighting function to condense the pointwise cross sections into groups. Afterwards, a one-dimensional flux calculation is done with a transport theory in cylindrical or slab geometry and in 70 energy groups, in all zones of the cell. Then the cross sections of the cell are condensed spatially as well as energetically. The cross section library is primarily based on JEF-1 evaluated data file.

Two-dimensional modules:

The configuration is represented by a X-Y mesh grid. Fuel and water cells are represented explicitly. The flux distribution can be calculated by either diffusion or a transport module. The results are the multiplication factor - keff, neutron flux, power distribution, and reaction rates.

Burnup module:

The evolution of isotopic densities for each material is calculated using reaction rates collapsed to one group by weighting with the multigroup fluxes from the cell- and the two-dimensional calculations. The time dependence of the nuclide densities is described by Taylor series. The nuclide densities with high destruction rates are assumed to be asymptotic. An iterative correction adjusts the fluxes within the time step in order to keep the power constant. The effect of the

changing spectrum on the reaction rates is taken into account by a predictor-corrector method and by density dependent one-group cross sections within the time step for ^{239}Pu and ^{240}Pu (approximated by a rational function). In the predictor-corrector method, the depletion is performed twice – using the spectrum at the beginning and at the end of the timestep. Average isotope number densities between these two calculations are then used as initial values for the subsequent burnup step. A time step can be divided into several micro-steps without recalculating the reaction rates in order to improve the numerical accuracy of the depletion calculation.

MCNP [3] is a general purpose Monte Carlo particles transport code developed at Los Alamos National Laboratory. It can be used in neutron, photon or electron transport mode as well as in a mode which is any combination of the above three. In the Monte Carlo approach, unlike in deterministic methods, the particles transport problem is solved by following the histories of individual particles. The average particle characteristics in the physical system are determined by average behavior of simulated particles. The major advantage of Monte Carlo method is its capabilities of solving a particle transport problem in complex generalized 3-D geometries which cannot be practically handled by deterministic methods. In principle, Monte Carlo simulation can yield the exact transport equation solution provided that physical models, nuclear data, and number of particle histories are sufficient. The major drawback of the Monte Carlo is considerably higher computation power requirements to achieve high accuracy of the results.

MNCP provides great flexibility in definition of particles source distributions, system geometries and tallied parameters. The energy deposition tally allows calculation of spatial power distribution in the modeled system. Dose rates can be calculated through surface flux or point detector tallies with provided flux-to-dose conversion factors. Calculation of k_{eff} eigenvalue is also a standard feature of MCNP.

III. Scope of Calculations

Two benchmark cases were evaluated using BOXER and MCNP computer codes: fuel unit cell and 17x17 pins standard PWR fuel assembly.

The objectives of the unit cell benchmark exercise are to calculate and compare neutron multiplication factor (k_{inf}) and isotopic reaction rates calculated by BOXER and MCNP codes in standard fuel unit cell geometry.

The objectives of the fuel assembly benchmark case are to compare the neutron multiplication factor (k_{inf}) and the local pin-by-pin power distribution.

IV. Unit cell benchmark

Six different cases were calculated in the unit cell benchmark. These cases differ in Pu loading, computer codes and cross section libraries used for the calculations.

Table 1 presents the list of all considered cases. BOXER code with JEF-1.1 library results are compared with those obtained with MCNP code using JEF-2.2 and JEF-3 cross section libraries.

The benchmark was performed for homogeneously mixed PuO_2-ZrO_2-MgO fuel. The Pu isotopic vector corresponds to that of a typical spent LWR fuel (UO_2, 4.2 w/o ^{235}U initial enrichment, 50 GWd/t discharge burnup, after 10 years of cooling)[4]. The detailed fuel composition is summarized in Table 2. The PWR pin-cell geometry and the operating conditions are shown in Table 3.

Table 1: List of calculated cases

Case number	Pu loading	Computer code	Cross section liabrary
1	5 v/o	BOXER	JEF-1.1
2	5 v/o	MCNP	JEF-2.2
3	5 v/o	MCNP	JEF-3
4	10 v/o	BOXER	JEF-1.1
5	10 v/o	MCNP	JEF-2.2
6	10 v/o	MCNP	JEF-3
7	15 v/o	BOXER	JEF-1.1
8	15 v/o	MCNP	JEF-2.2
9	15 v/o	MCNP	JEF-3

Table 2: Fuel composition for benchmark calculations

Fuel Component	Theoretical Density [5] (g/cm^3)	Density used for the exercise (g/cm^3)	Volume Fraction		
			Case 1	Case 2	Case 3
PuO_2	11.46	10.77	0.05	0.100	0.150
ZrO_2	5.68	5.68	0.475	0.450	0.425
MgO	3.65	3.65	0.475	0.450	0.425
Isotope	**Number density #/(cm × barn)**	**Initial Pu vector [4] w/o of total Pu**			
Pu238	7.65E-05	0.0318			
Pu239	1.35E-03	0.5635			
Pu240	6.35E-04	0.2662			
Pu241	1.91E-04	0.0802			
Pu242	1.38E-04	0.0583			
Zr (Nat.)	1.25E-02				
Mg (Nat.)	2.45E-02				
O (Nat.)	5.43E-02				

Table 3: Pin cell operating conditions and geometry

Fuel pellet radius (cm)	0.4095
Cladding outer radius (cm)	0.4750
Pin Pitch (cm)	1.26
Cladding material	Zr_{nat}
Cladding density (g/cm^3)	6.43
Coolant density (g/cm^3)	1.0035
Fuel temperature (K)	300
Coolant temperature (K)	300

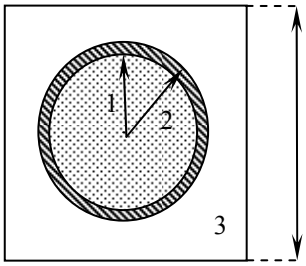

Region	Material
1	Fuel
2	Cladding
3	Water

Top view of fuel pin cell

The results of the unit cell benchmark calculations are summarized in Tables 4 through 7. Table 4 compares the k-infinity values predicted by BOXER and MCNP codes. The discrepancy in k eigenvalue prediction between the BOXER and MCNP (JEF-2.2) is on the order of 0.2%. The difference between the BOXER and MCNP with more recent JEF-3 library is slightly higher (up to 0.37%). Such differences are generally acceptable for the scoping calculations, conceptual design, and preliminary feasibility studies. Thus, results shown in Table 4 demonstrate validity of the boxer code for the purposes of the current analyses. It should also be noted that the difference in k-infinity values is reduced with an increase in Pu loading.

Tables 5 through 7 compare absorption and fission reaction rates for all 6 calculated unit cell cases. All reaction rates values are extracted for the fuel region only. The following can be observed from the results.

- The main contributors to the differences in criticality and reaction rates are Zirconium and Pu240, Pu241, and Pu242 isotopes. Part of the differences is compensating, resulting in a relatively small $\Delta\rho$ values.
- One of the major sources of discrepancy in k-infinity predictions is the uncertainty in natural Zr cross section data resulting in difference in Zr absorption rates of up to 0.17%. BOXER values are consistently higher than those of MCNP. Thus, from the criticality point of view BOXER results are conservative.
- BOXER JEF-1.1 library results for Zr absorption rates agree better with the latest JEF-3 library than with JEF-2.2 as illustrated by Figure 1, which compares the absorption reaction rates in 70 energy groups in Zr for the Cases 4, 5, and 6.
- The discrepancy in Zr absorption rate prediction reduces with an increase in Pu loading and the resulting neutron spectrum changes, which may be attributed to the compensating effect mentioned above. Figure 2 shows significant decrease in thermal neutron flux for the cases with higher Pu loading. For consistency, the total neutron flux is normalized to unity in all cases.
- Another source of discrepancy in k-infinity prediction originates in differences in absorption rates in Pu240 and Pu242 isotopes in BOXER-MCNP(JEF-2.2) comparison and in Pu241 isotope in BOXER-MCNP(JEF-3) comparison.
- Fission reaction rates in Pu240 and Pu242 isotopes have notable discrepancy particularly in the epithermal energy range as can be observed from Figure 3 and Figure 4. Although overall the contribution of fission reactions in these isotopes to total absorption is small (Figure 5 and Figure 6) leading to only marginal effect on criticality prediction.

Table 4: Neutron multiplication factor (unit cell)

	K-INF Boxer (JEF1.1)	K-INF MCNP (JEF2.2)	K-INF MCNP (JEF3)	Δρ (BOXER – JEF2.2)	Δρ (BOXER – JEF3)
Case 1	1.44073	1.43600±0.00066	1.43305±0.00064	0.23%	0.37%
Case 2	1.43013	1.42686±0.00073	1.42425±0.00081	0.16%	0.29%
Case 3	1.43821	1.43554±0.00078	1.43488±0.00071	0.13%	0.16%

Table 5: One group normalized reaction rates (Case1)

Nuclide	Fission rates			Total absorption rates			difference in total absorbtion	
	BOXER (JEF1.1)	MCNP (JEF2.2)	MCNP (JEF3)	BOXER (JEF1.1)	MCNP (JEF2.2)	MCNP (JEF3)	(BOXER-JEF2.2)	(BOXER-JEF3)
O_{16}				2.35E-03	3.15E-03	3.00E-03	-0.080%	-0.065%
Mg_{nat}				1.74E-03	1.76E-03	2.09E-03	-0.002%	-0.035%
Zr_{nat}				6.92E-03	5.23E-03	6.29E-03	0.169%	0.063%
Pu_{238}	1.06E-03	1.06E-03	1.16E-03	1.17E-02	1.17E-02	1.18E-02	-0.001%	-0.009%
Pu_{239}	4.38E-01	4.37E-01	4.38E-01	6.59E-01	6.59E-01	6.59E-01	0.029%	-0.037%
Pu_{240}	2.49E-03	2.54E-03	2.42E-03	1.96E-01	1.97E-01	1.96E-01	-0.120%	0.019%
Pu_{241}	7.87E-02	7.83E-02	7.69E-02	1.05E-01	1.04E-01	1.03E-01	0.091%	0.150%
Pu_{242}	4.10E-04	4.19E-04	4.21E-04	1.76E-02	1.85E-02	1.85E-02	-0.086%	-0.085%
Total	5.21E-01	5.19E-01	5.19E-01	1.00E+00	1.00E+00	1.00E+00	0.000%	0.000%

Table 6: One group normalized reaction rates (Case 2)

Nuclide	Fission rates			Total absorption rates			difference in total absorbtion	
	BOXER (JEF1)	MCNP (JEF2.2)	MCNP (JEF3)	BOXER (JEF1)	MCNP (JEF2.2)	MCNP (JEF3)	(BOXER-JEF2.2)	(BOXER-JEF3)
O_{16}				2.29E-03	3.06E-03	2.94E-03	-0.077%	-0.065%
Mg_{nat}				1.13E-03	1.14E-03	1.47E-03	-0.001%	-0.033%
Zr_{nat}				5.55E-03	4.09E-03	5.04E-03	0.146%	0.051%
Pu_{238}	1.69E-03	1.71E-03	1.88E-03	1.17E-02	1.18E-02	1.21E-02	-0.004%	-0.035%
Pu_{239}	4.20E-01	4.18E-01	4.20E-01	6.36E-01	6.36E-01	6.36E-01	-0.001%	-0.027%
Pu_{240}	4.79E-03	4.86E-03	4.66E-03	2.11E-01	2.12E-01	2.11E-01	-0.115%	0.025%
Pu_{241}	8.22E-02	8.19E-02	8.04E-02	1.09E-01	1.08E-01	1.07E-01	0.115%	0.162%
Pu_{242}	7.93E-04	8.07E-04	8.20E-04	2.32E-02	2.38E-02	2.39E-02	-0.063%	-0.078%
Total	5.09E-01	5.08E-01	5.07E-01	1.00E+00	1.00E+00	1.00E+00	0.000%	0.000%

Table 7: One group normalized reaction rates (Case 3)

Nuclide	Fission rates			Total absorption rates			difference in total absorbtion	
	BOXER (JEF1)	MCNP (JEF2.2)	MCNP (JEF3)	BOXER (JEF1)	MCNP (JEF2.2)	MCNP (JEF3)	(BOXER-JEF2.2)	(BOXER-JEF3)
O_{16}				2.26E-03	3.03E-03	2.91E-03	-0.078%	-0.065%
Mg_{nat}				9.18E-04	9.30E-04	1.24E-03	-0.001%	-0.032%
Zr_{nat}				4.89E-03	3.56E-03	4.40E-03	0.132%	0.048%
Pu_{238}	2.32E-03	2.33E-03	2.59E-03	1.25E-02	1.25E-02	1.30E-02	-0.006%	-0.052%
Pu_{239}	4.11E-01	4.09E-01	4.11E-01	6.23E-01	6.22E-01	6.23E-01	0.143%	-0.019%
Pu_{240}	7.02E-03	7.12E-03	6.87E-03	2.16E-01	2.18E-01	2.16E-01	-0.255%	0.000%
Pu_{241}	8.73E-02	8.69E-02	8.55E-02	1.15E-01	1.13E-01	1.13E-01	0.163%	0.186%
Pu_{242}	1.17E-03	1.19E-03	1.21E-03	2.61E-02	2.70E-02	2.67E-02	-0.099%	-0.065%
Total	5.09E-01	5.06E-01	5.07E-01	1.00E+00	1.00E+00	1.00E+00	0.000%	0.000%

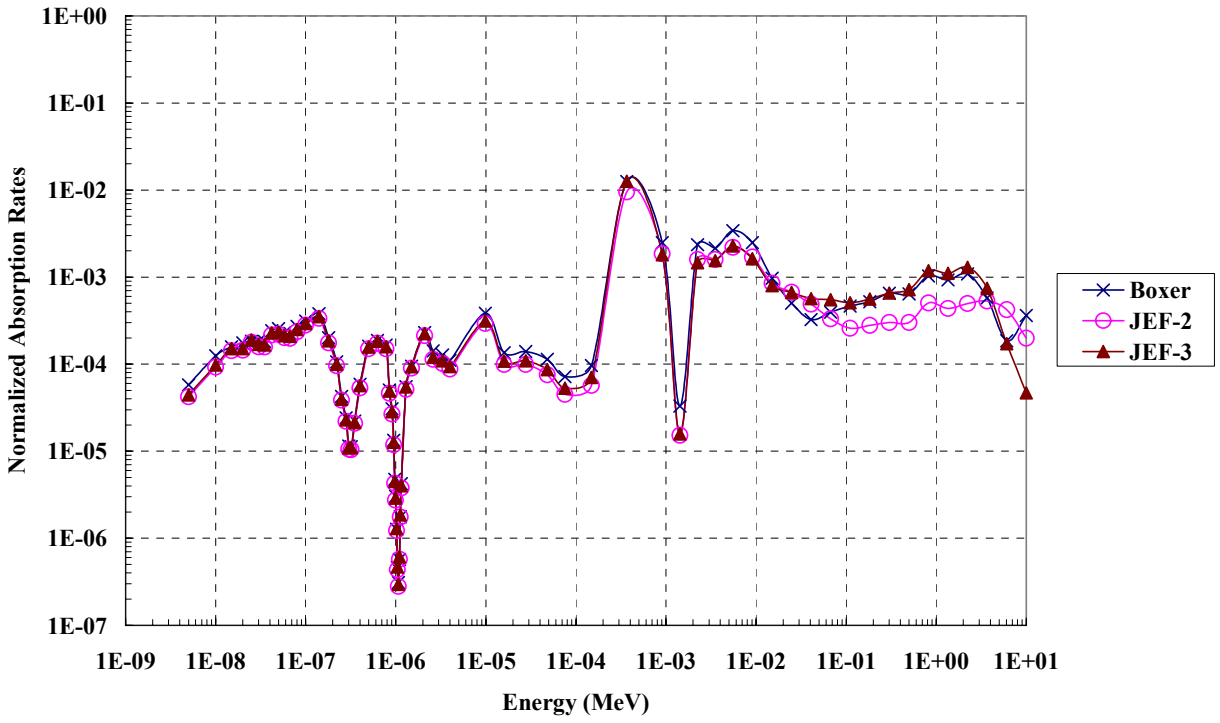

Figure 1: Absorption rates in Zr in 70 energy groups

Note: non-negligible difference in the high energy range 10KeV – 2MeV

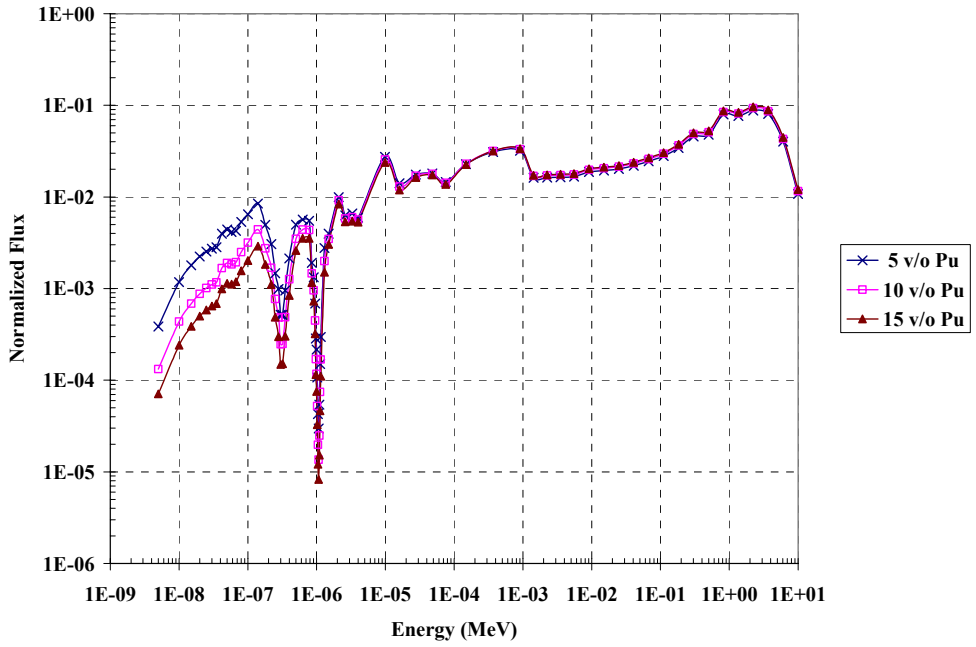

Figure 2: Neutron Energy Spectrum in 70 groups

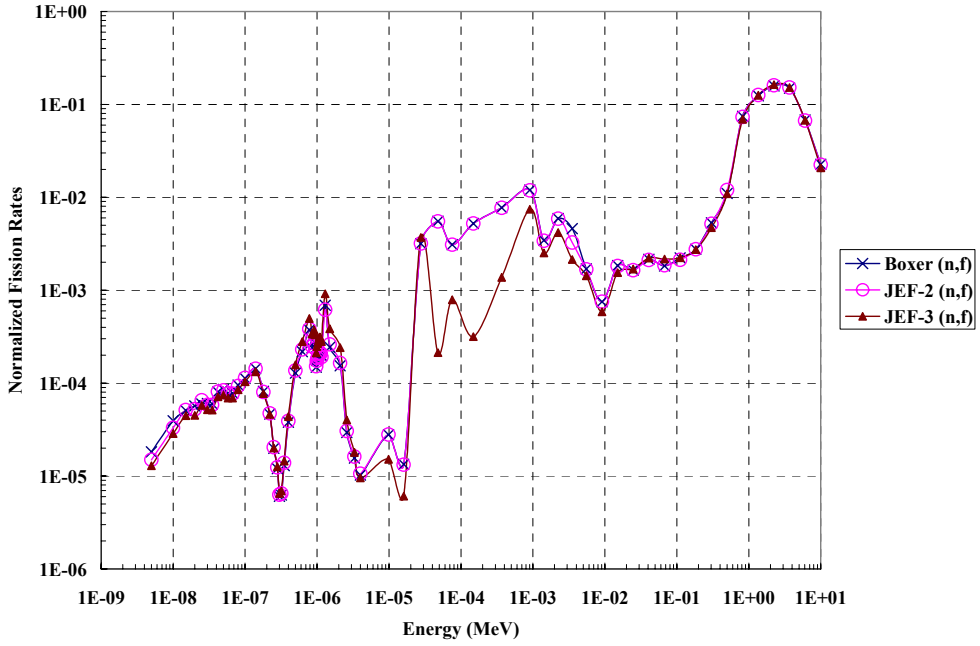

Figure 3: Fission rates in Pu240 in 70 energy groups (10 v/o PuO_2 loading)

Note: Good agreement between BOXER (JEF-1.1) and MCNP (JEF-2.2) while significant discrepancy between former two and MCNP (JEF-3) in the energy range 20eV – 1KeV

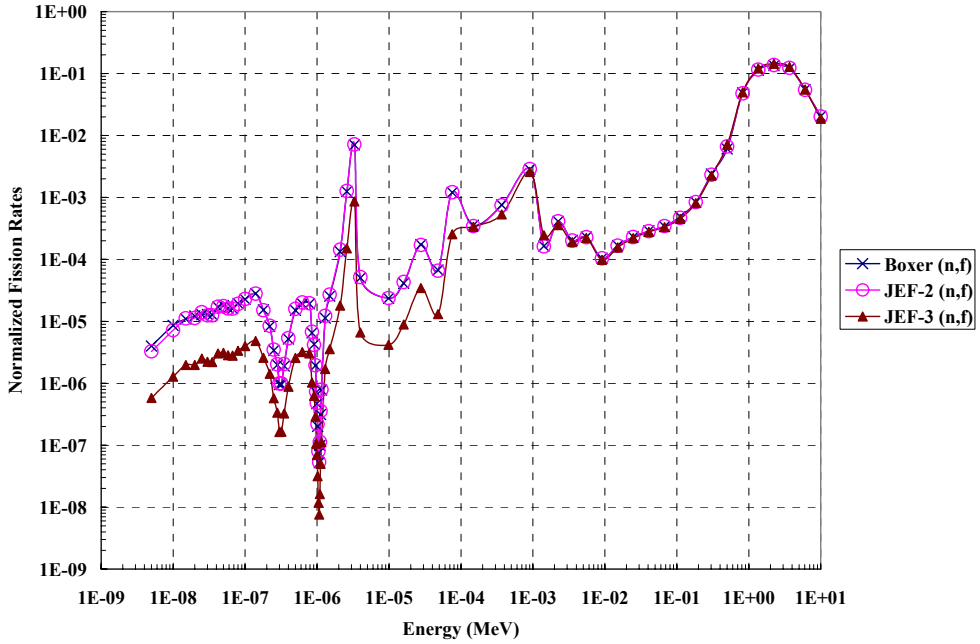

Figure 4: Fission rates in Pu242 in 70 energy groups (10 v/o PuO_2 loading)

Note: Good agreement between BOXER (JEF-1.1) and MCNP (JEF-2.2) while significant discrepancy between former two and MCNP (JEF-3) in the energy range 0.001eV – 1KeV

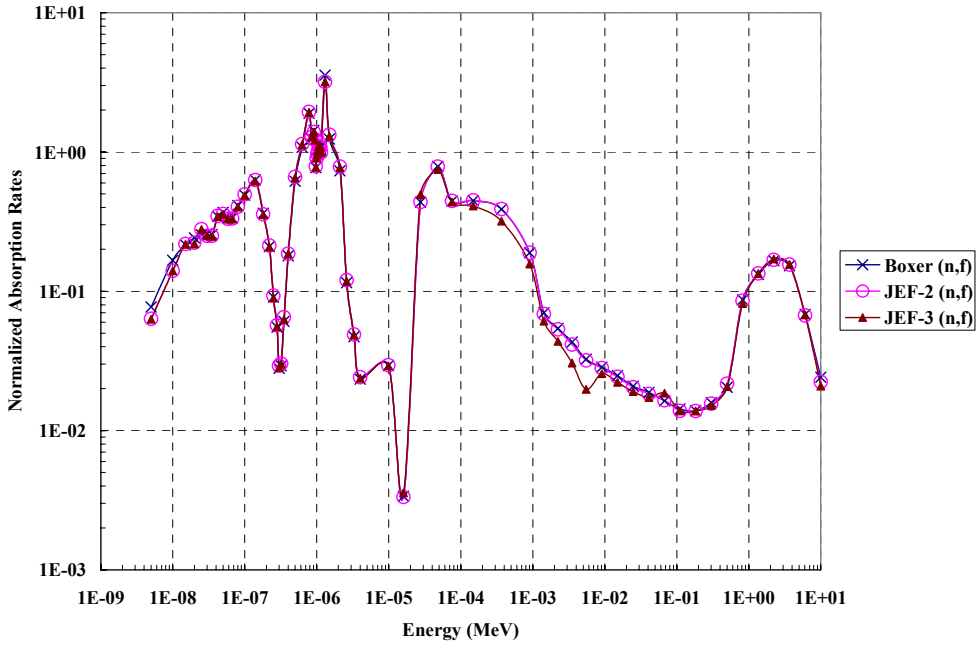

Figure 5: Absorption rates in Pu240 in 70 energy groups (10 v/o PuO_2 loading)

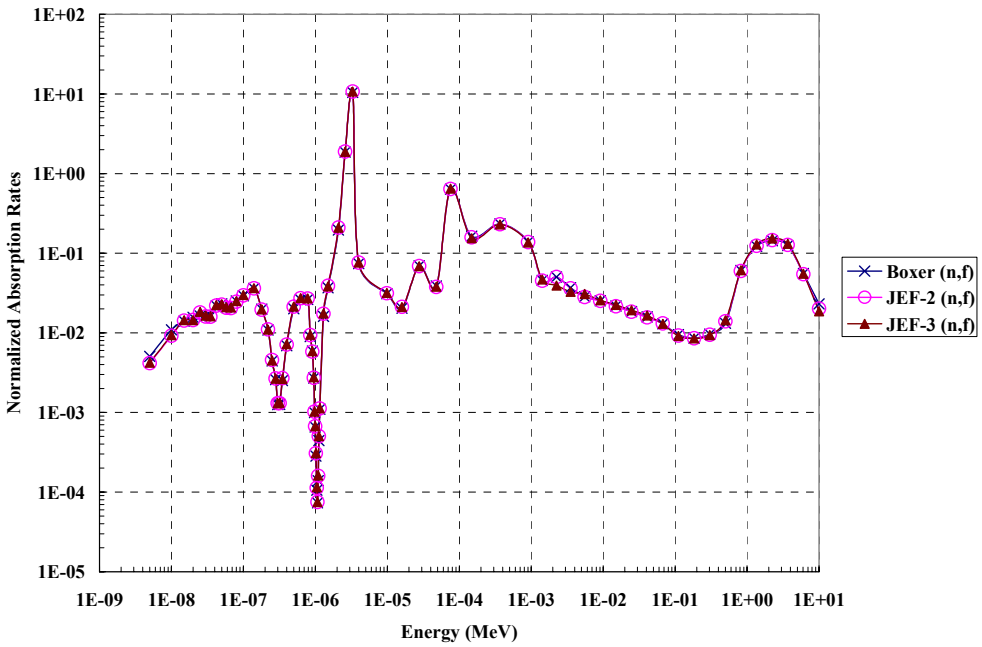

Figure 6: Absorption rates in Pu242 in 70 energy groups (10 v/o PuO_2 loading)

V. PWR Fuel assembly benchmark

In this part of the benchmark, the 2D transport calculations were performed for a typical 17 X 17 PWR fuel assembly. The assembly consists of 264 fuel rods and 25 guide tubes. The fuel unit cell geometry and material composition are identical to those used in the unit cell benchmark case and presented in Table 2 and Table 3. The fuel assembly geometry description and operating conditions are presented in Table 8. The BOXER calculations were performed for ¼ of PWR assembly with zero buckling and reflective boundary conditions. In the MCNP calculations, the octant symmetry also with reflective boundary conditions was used to simplify the model.

Figure 7 depicts the MCNP model geometry used for the benchmark. Direct fission heating and γ-smearing were considered in both codes. ENDF-B/VI data library was used in MCNP.

Table 8: Summary of fuel assembly parameters

Operating parameter	Value
Assembly array	17 X 17
Array geometry	Square
Number of fuel rods per assembly	264
Assembly pitch (cm)	21.5
Interassembly water gap (cm)	0.04
Fuel pin pitch, cm	1.26
Guide tube inner radius (cm)	0.5715
Guide tube outer radius (cm)	0.6120
Guide tube cladding material	Zr_{nat}
Guide tube cladding density (g/cm^3)	6.43
Fuel temperature, K	900
Moderator temperature, K	583
System pressure, bar	155

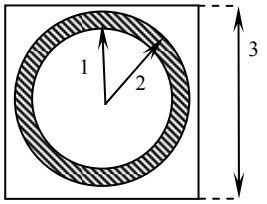

Region	Material
1	Water
2	Cladding
3	Water

Top view of guide tube

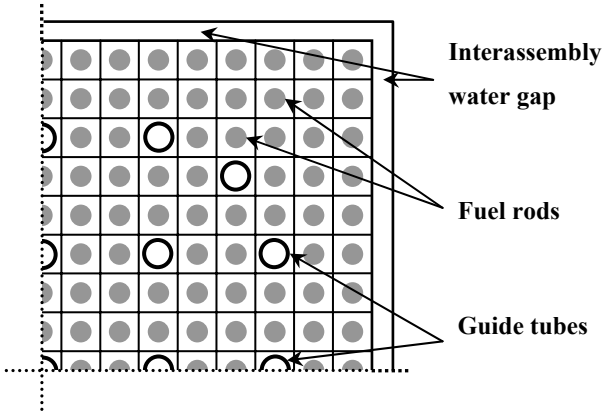

The north-east fourth of assembly

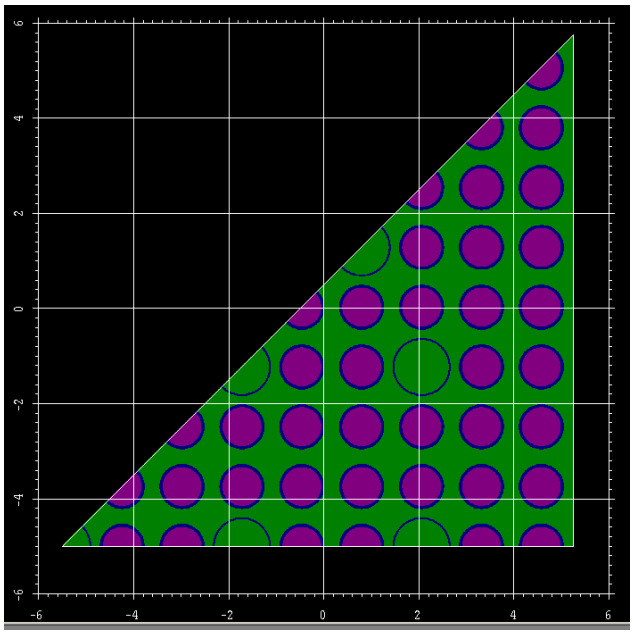

Figure 7: MCNP calculation model of PWR assembly

The results of PWR assembly benchmark calculations are presented in Table 9 and in Figure 8. As in the unit cell benchmark, sufficiently good agreement (0.23% Δρ) was obtained for the criticality prediction. The pin-by-pin power distribution was predicted with less than 2% differences between the two codes. Both codes identified the hot fuel pin at the same location.

Table 9: Neutron multiplication factor (assembly)

	BOXER	**MCNP**
K-INF	1.38983	1.38600 ± 0.00061
Δρ	0.23%	

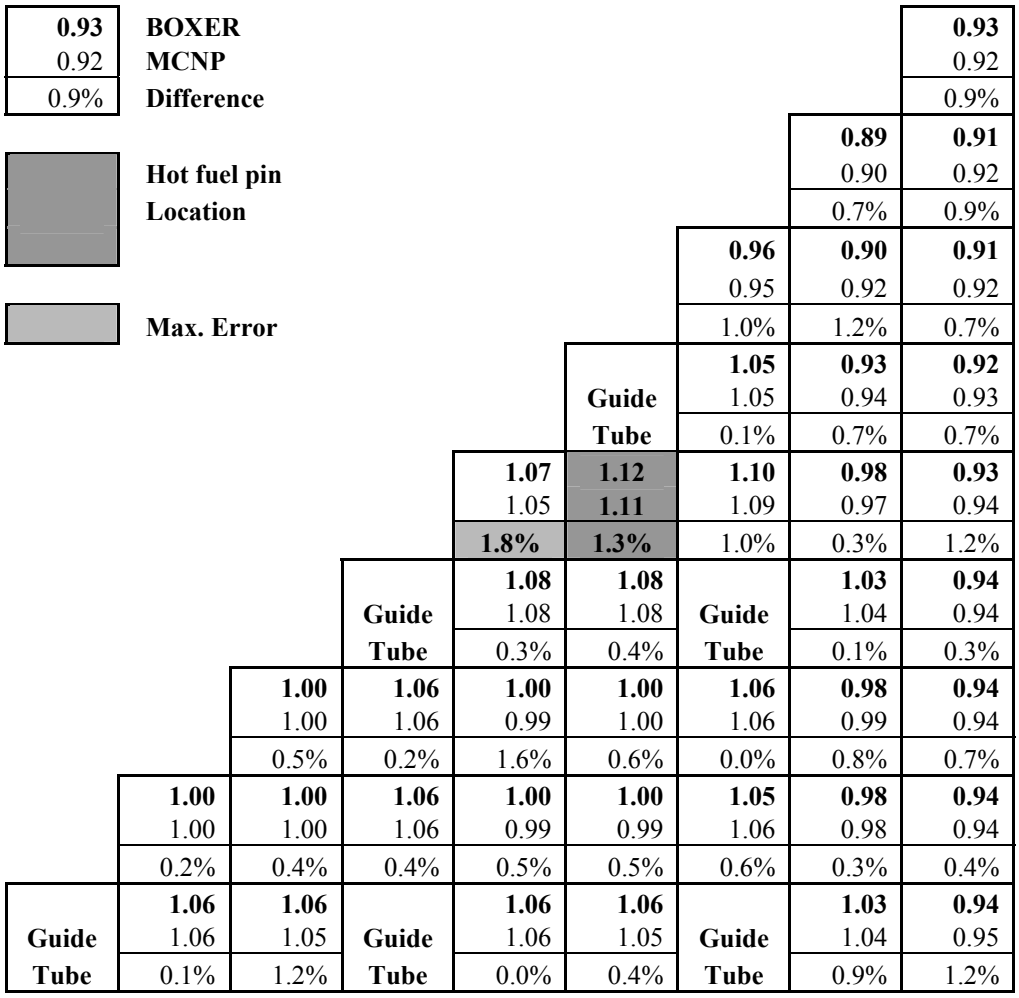

Figure 8: Pin-by-pin relative power distribution in PWR fuel assembly

VI. Summary and Conclusions

We performed a number of benchmark calculations for a standard PWR unit cell and 17x17 fuel assembly. The results of the BOXER computer code, suggested for use in the analysis of fertile free matrix fuels, were compared with MCNP results for different Pu loadings and cross section libraries. The criticality prediction difference between BOXER and MCNP ranges between 0.13 and 0.37% depending on the cross section library and Pu loading. The absorption

rates in Zr, Pu240 and Pu242 isotopes were identified as major contributors to the discrepancy in criticality prediction. Relatively large Zr contribution to the total k-infinity prediction difference is due to the large Zr concentration in the fuel matrix as compared to a typical UO_2 fuel where Zr presents only in the cladding. The relative error introduced by the Zr cross section data uncertainty decreases with an increase of Pu v/o and related hardening of the neutron spectrum. This is expected to introduce additional uncertainty in evaluation of Moderator Temperature and Void reactivity feedback coefficients as pointed out in Reference 6. Validation of BOXER computer code with respect to the accuracy of reactivity coefficients evaluation necessary for performing Task 3 of this program will be performed in the next stage. Analysis of the energy dependent differences for major isotopes presented in this report will provide a starting point for these studies.

The fuel assembly benchmark case tested the capabilities of 2D transport module of the BOXER code. We observed reasonable agreement in criticality prediction of the standard 17x17 PWR fuel assembly between BOXER and MCNP - on the order of 0.2% $\Delta\rho$. The fuel assembly local pin power distribution predicted by the two codes is within 2% discrepancy.

In conclusion, the performed benchmark calculations confirmed that the BOXER code is suitable for the scoping studies of plutonium in fertile free matrix fuel designs. The BOXER code predicts criticality, reaction rates and power distribution in fuel assembly with accuracy sufficient for the purposes of this study.

References

[1] Paratte J.M., Foskolos K., Grimm P., and Maeder C., "Das PSI Codesystem ELCOS zur stationaren Berechnung von Leichtwasserreaktoren", Proc. Jahrestagung Kerntechnik, Travemunde, p.59, Germany, May 17-19 (1988)

[2] Paratte J.M., Grimm P., and Hollard J.M., "User's Manual for the Fuel Assembly Code BOXER", PSI, CH-5232 Villingen PSI, (1995)

[3] Briesmeister J. F. (editor), "MCNP™ - A General Monte Carlo N-Particle Transport Code, Version 4C," LA-13709M, Los Alamos National Laboratory, April (2000).

[4] Van Tuyle G.J., "Candidate Approaches for an Integrated Nuclear Waste Management Strategy - Scoping Evaluations", Los Alamos National Laboratory, LA-UR-01-5572, (2001).

[5] CRC Press, "Properties of Inorganic Compounds", CRC Handbook of Chemistry and Physics, 3rd Electronic Edition, (2000) (http://www.knovel.com)

[6] Baldi S., Porta J., Peneleau Y., Pelloni S., Paratte J.-M., Chawla R., "Importance of zirconium cross sections in calculating reactivity effects for inert matrix fuels," *Progress in Nuclear Energy*, **38**, 3-4, pp. 351-354, (2001).